THE LUNAR OCCULTATION OF THE CRAB NEBULA OBSERVED AT PARKES ON JUNE 21, 1963

By R. D. DAVIES,*† F. F. GARDNER,* C. HAZARD,‡ and M. B. MACKEY*§

[*Manuscript received January* 24, 1966]

Summary

Measurements of the intensity and percentage linear polarization of the Crab nebula radiation at 404 and 1420 Mc/s were made during the partial occultation of June 21, 1963. The radio occultation curves are similar in shape to that calculated from the isophotes of the optical continuum and show the same principal features. However, the ratio of radio to optical brightness varies in a systematic way across the source, the ratio being greater at the edges than in the central regions. This steepening of the spectral index towards the outer edges continues in the radio frequency range from 1420 to 404 Mc/s. The 1420 Mc/s linear polarization is stronger in the inner areas (2·5%) than in the outer areas (< 1%) of the source.

I. INTRODUCTION

An occultation of the Crab nebula by the Moon was observed with the 210 ft radio telescope at Parkes, N.S.W., on June 21, 1963. Although this was a partial occultation in which about 80% of the radio emission was occulted, the circumstance of the occultation was such that any bright sources within the occulted area would be accurately located. Measurements were made at 404 and 1420 Mc/s in an attempt to find any change in the brightness distribution with frequency. These data were then used in conjunction with optical brightness contours published by Woltjer (1957) to obtain a comparison of the optical and radio distribution in the Crab nebula. In addition, detailed linear polarization measurements were made at both frequencies during the occultation in an attempt to reconstruct the polarization distribution within the Crab nebula.

II. METHOD OF OBSERVATION

The observations were carried out at frequencies of 404 and 1420 Mc/s using unswitched, double-sideband receivers with crystal mixer input stages. At 404 Mc/s the two sidebands were 8 Mc/s wide and centred 10 Mc/s on either side of the central frequency, while at 1420 Mc/s the sidebands were 10 Mc/s wide and centred 30 Mc/s on either side of the central frequency. The effective input temperatures of the receivers were 500°K and 800°K at 404 and 1420 Mc/s respectively. The aerial temperatures due to the Crab were 500°K and 400°K.

* Division of Radiophysics, CSIRO, University Grounds, Chippendale, N.S.W.

† Present address: Nuffield Radio Astronomy Laboratories, Jodrell Bank, England.

‡ School of Physics, University of Sydney; present address: Ionospheric Observatory, Arecibo, Puerto Rico.

§ Present address: Standard Telephones and Cables, Sydney.

The position of the Crab was measured at 1420 Mc/s to be R.A. $05^h\,32^m\,19^s$, Dec. $+21°\,59'{\cdot}7$ as read on the telescope dials, which have an absolute accuracy of better than $\pm 1'$ arc in either coordinate. As the half-power beamwidth of the telescope was 14′ arc at 1420 Mc/s and 48′ arc at 404 Mc/s, source intensity changes produced by tracking errors were negligible. The short-term following was accurate to better than 5″ arc, and fluctuations in the Moon's contribution to the overall intensity were less than those imposed by noise fluctuations, even at 1420 Mc/s. The source was tracked from $00^h\,46^m$ U.T. to $03^h\,25^m$ U.T., and the received power at each frequency was displayed on a pen recorder. The receiver time constant was 1 sec. Linear polarization measurements throughout the whole tracking period were made by setting the combined 404 and 1420 Mc/s primary feed antenna at feed angles of 0°, 45°, 90°, and 135° in turn and repeating the sequence of feed angles about twice per minute.

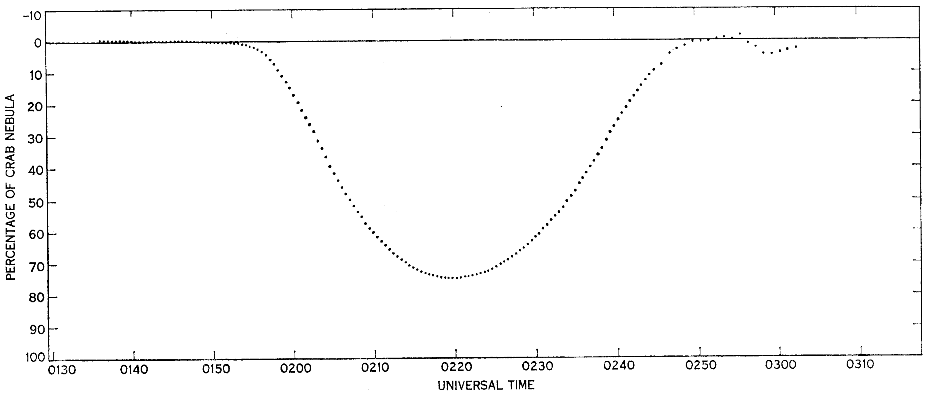

Fig. 1.—The 404 Mc/s occultation curve of the Crab nebula expressed as a percentage of the unocculted source. Corrections have been made for the contribution from the Moon.

At each frequency, mean values of the intensities at the four feed angles were obtained at half-minute intervals during the occultation. The mean values were then corrected for the nonlinearity of the receivers over the large intensity range covered and for the Moon's contribution to the received power. The contribution due to the Moon at each frequency was evaluated from a scan made on the previous day across the Moon along the same chord as that traversed by the centre of the beam during the occultation.

III. Results and Comparison with Optical Data

(a) *404 Mc/s Observations*

At 404 Mc/s, the Moon's contribution at the centre of the occultation was only $1{\cdot}4\%$ of the unocculted flux from the Crab nebula. Figure 1 shows the mean corrected intensity of the Crab during the occultation, expressed as a percentage of the unocculted intensity; at the centre, $75(\pm 1)\%$ of the source was occulted.

The observed polarization at the beginning of the occultation was $0{\cdot}6\%$ of the unocculted intensity, falling to $0{\cdot}3\%$ at the centre of the occultation. However, these figures may not be significant, since on June 21, 1963, the Sun was only 23·5 solar radii away from the Crab, and at this distance it can give rise to appreciable spurious polarization effects, as well as occasional short-period fluctuations in intensity with periods of 1 to 10 sec which are thought to be caused by scattering of the radiation by particle clouds emitted by the Sun.

During the occultation, the short-period intensity variations were small ($\leqslant 0\cdot15\%$) until $02^{h}\,43^{m}$ when the level of the received power became increasingly variable, reaching 4% at $02^{h}\,51^{m}$ and later. This may have included some terrestrial interference reflected from the Moon. Consequently, the 404 Mc/s occultation curve is unreliable after $02^{h}\,43^{m}$. The reference level of the curve at emersion was taken as the mean level observed between $02^{h}\,54^{m}$ and $03^{h}\,00^{m}$ U.T.

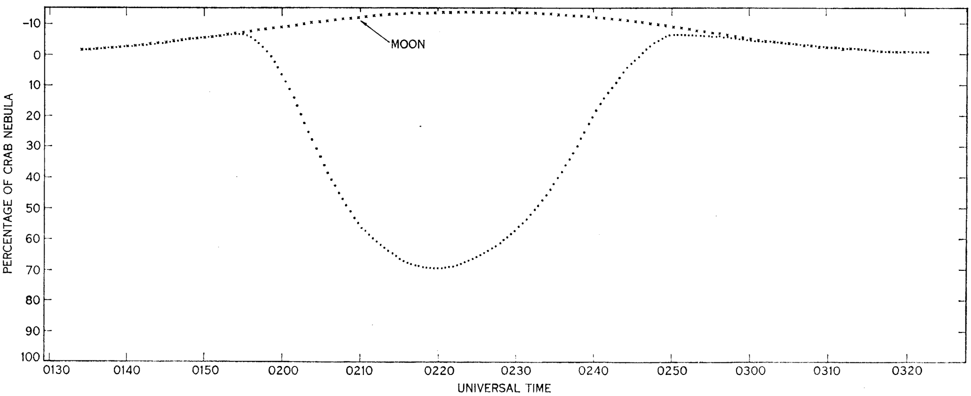

Fig. 2.—The observed 1420 Mc/s occultation curve of the Crab nebula expressed as a percentage of the unocculted source.

(*b*) *1420 Mc/s Observations*

The 1420 Mc/s intensities, corrected in the same way as the 404 Mc/s values, are plotted at each 0·5 min interval, throughout the period of the occultation, in Figure 2. A steady baseline drift of 3% of the intensity of the source, which occurred over a period of 2 hr on either side of the occultation maximum, was removed from the data before plotting. The variation in received power due to the passage of the Moon through the aerial beam, derived from measurements made the previous day, is also plotted in Figure 2. The true occultation curve is the difference between these two curves. At the minimum, 83($\pm$3)% of the source was occulted.

The variation of the linear polarization during the occultation is plotted vectorially in Figure 3(*a*). Each point gives the polarized intensity derived from the sine wave with an angular period of 180° fitted to the four intensity values at feed angles of 0°, 45°, 90°, and 135°. The position angle of the polarization is the feed angle of maximum intensity plus the parallactic angle. The polarized intensity is expressed for convenience as a percentage of the flux from the unocculted source. The Moon is also a polarized source, and its distribution has been measured with the 14′ beam at 1420 Mc/s (Davies and Gardner, paper in preparation); its contribution

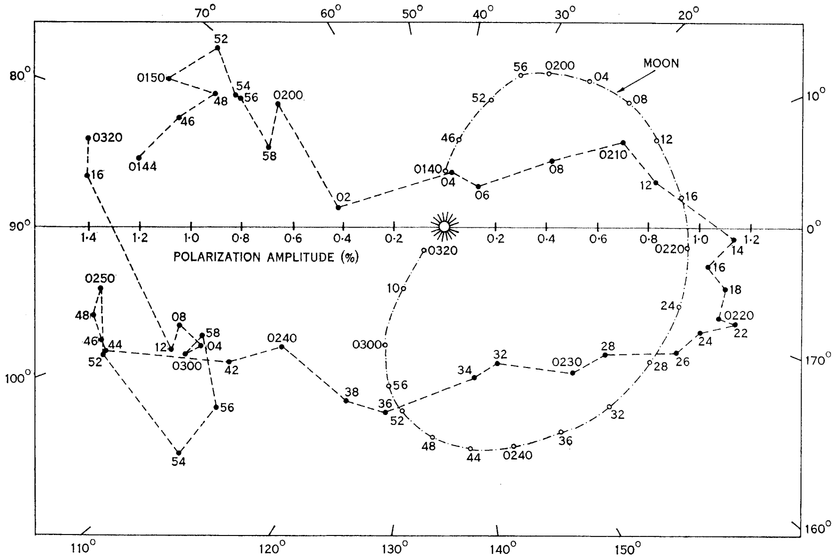

Fig. 3(*a*).—A vectorial plot of the observed 1420 Mc/s linear polarization every 2 min of U.T. during the occultation. The contribution from the Moon estimated at intervals over the same period is also shown. In both plots the polarization intensity is given as a percentage of the unocculted source.

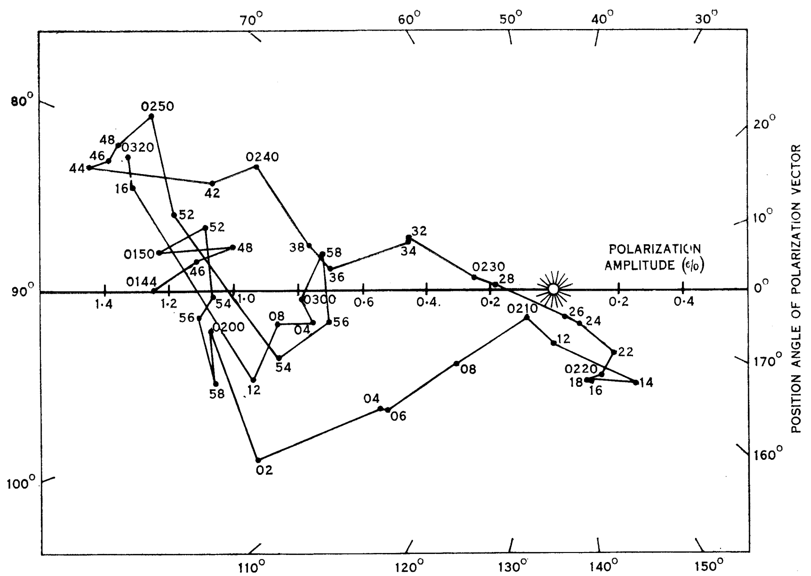

Fig. 3(*b*).—The vectorial plot of the polarization corrected for the contribution of the Moon during the occultation.

to the observed polarization was derived from scans made the previous day, and this is also plotted in Figure 3(*a*). Since the angles plotted in the figure are twice the polarization angle, the true variation of polarization through the occultation is the vector difference between these two plots, and this is shown in Figure 3(*b*). The Stokes parameters Q and U at each point are the orthogonal components of the vectors.

The random error at each point is estimated to be $0 \cdot 07\%$ and would be represented on the plots by a circle of this radius centred on each point. In addition to these observational errors, larger spurious polarization effects occur occasionally

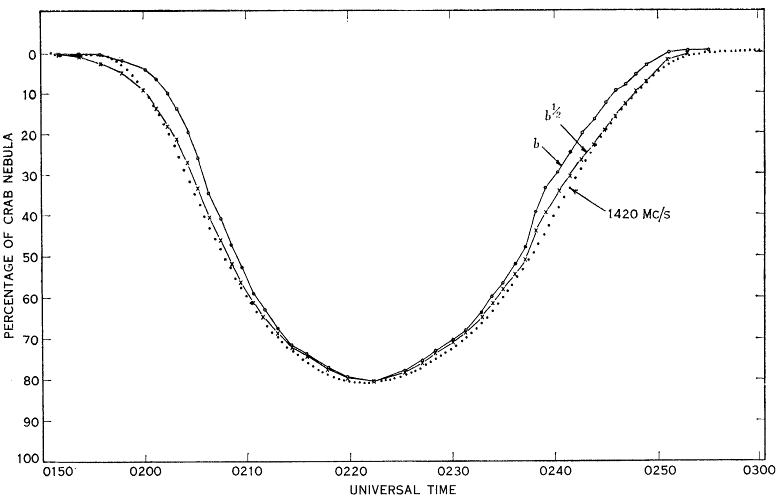

Fig. 4.—The corrected 1420 Mc/s occultation curve compared with the occultation curve of the optical brightness distribution b and $b^{\frac{1}{2}}$. All curves have been normalized to the 1420 Mc/s percentage occultation (83%) at the centre of the occultation.

near the Sun. Previous experience had shown that these effects and the intensity variations mentioned previously were much smaller at 1420 Mc/s than at 404 Mc/s. The possibility of a small residual effect on the 1420 Mc/s polarization will be considered in Section III(*e*).

(*c*) *Comparison with Optical Intensity Data*

The radio occultation curves are compared with the optical occultation curve calculated from the isophotes of photographic brightness of the continuum emission from the Crab nebula, in the wavelength range 5200 to 6400 Å, published by Woltjer (1957). To make this comparison, it was first necessary to obtain an accurate position for the optical object, and the double star near the centre of the Crab nebula was used as a point of reference. The mid point of the two stars as given by Seeger and Westerhout (1957) is

$$\text{R.A. } 05^{\text{h}}\,31^{\text{m}}\,31^{\text{s}}{\cdot}55, \quad \text{Dec. } +21^{\circ}\,58'\,56''{\cdot}88 \qquad (1950{\cdot}0).$$

At the time of observation, the precessed position was

$$\text{R.A. } 05^{\text{h}}\,32^{\text{m}}\,17^{\text{s}}\!\cdot\!45, \quad \text{Dec. } +21^{\circ}\,59'\,24''\!\cdot\!6 \qquad \text{(June 21, 1963).}$$

The path of the Moon and its apparent radius as observed from Parkes were calculated at intervals through the occultation by use of a computer program developed for radio source occultation work. Plate 1 shows the position of the limb of the Moon at 2 min intervals during the occultation, superimposed on contours of photographic brightness reproduced from a photograph published by Woltjer (1957).

The optical occultation curve was calculated by integrating over the unocculted contours at intervals of 1–2 min depending on the rate of change of integrated brightness. In addition, a second occultation curve corresponding to the square root of each of Woltjer's contour levels was calculated. These two optical curves are shown in Figure 4 and compared with the true occultation curve at 1420 Mc/s. For this comparison, the two optical curves were normalized so that 83% of the source was occulted at the maximum.

Three points are immediately obvious from Figure 4.

(1) The centre of the radio source agrees closely in position with the centre of the Crab nebula, a conclusion similar to that of Seeger and Westerhout (1957). Any displacement between the radio and optical curves would appear to correspond to a displacement in the two distributions of less than 4″ arc. Thus, the position of the radio centre may be taken as that of the optical centre given by Woltjer (1958), namely,

$$\text{R.A. } 05^{\text{h}}\,31^{\text{m}}\,30^{\text{s}}\!\cdot\!7 \pm 0^{\text{s}}\!\cdot\!4, \quad \text{Dec. } +21^{\circ}\,59'\,0''\!\cdot\!9 \pm 3'' \qquad (1950\cdot 0).$$

The errors represent the accuracy with which the radio and optical occultation curves can be aligned.

(2) The distribution of radio brightness is considerably flatter than the optical distribution; it corresponds more closely to the square root of the optical distribution.

(3) Although the radio brightness distribution is less highly concentrated towards the centre of the Crab nebula than the optical brightness distribution, the maximum extents of the two distributions are not greatly different.

A more sensitive method for comparing radio and optical features is to compare the differentials of the occultation curves. It can be seen from Plate 1 that, at immersion, the section of the Moon's limb covering the nebula defines an approximately straight line, at a position angle of about 110°, over the period $01^{\text{h}}\,50^{\text{m}}$ to about $02^{\text{h}}\,12^{\text{m}}$ U.T. Similarly, at emersion it defines an approximately straight edge, at a position angle of about 50°, from $02^{\text{h}}\,36^{\text{m}}$ to $02^{\text{h}}\,56^{\text{m}}$ U.T. Thus, in these two intervals, approximate strip distributions along these two position angles from the outer limits of the nebula to just beyond the central region are derived. The differential distributions of the intensities at optical and both radio frequencies are shown in Figure 5. They were obtained by measuring the changes in intensity between successive positions of the Moon's limb separated by 10″ arc. Figure 5 shows firstly that there is good agreement between the 1420 and 404 Mc/s strip distributions in their overall width and in most of the minor details. The effective fluctuation level

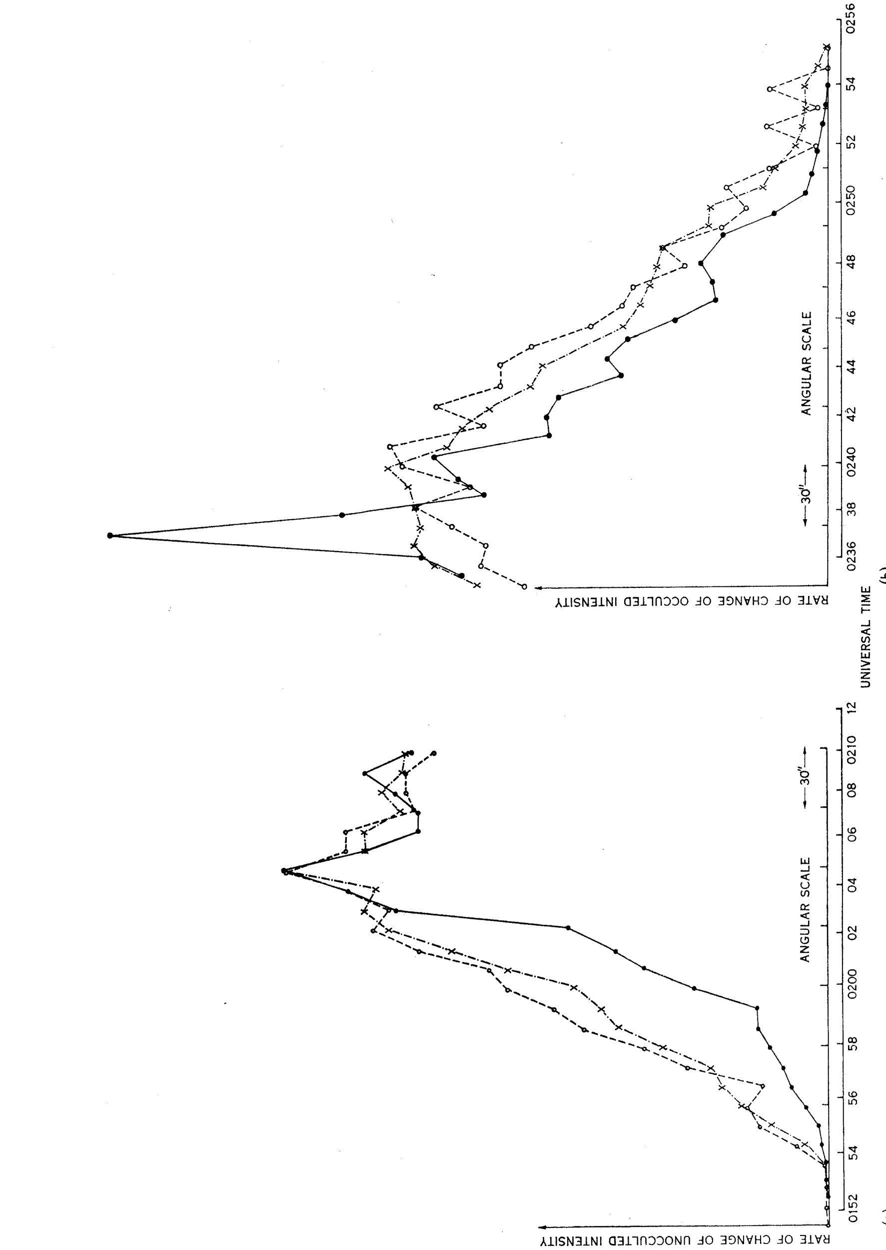

Fig. 5.—The differential brightness distribution across the Crab nebula (*a*) on immersion (*b*) on emersion, as derived from 404 Mc/s (- - - - -), 1420 Mc/s (-·-·-·-), and optical (———) data.

is about $\pm 1\%$ of the peak amplitude of Figure 5 at 1420 Mc/s, and about $\pm 2\%$ at 404 Mc/s, prior to about $02^h\,44^m$ when short-period intensity variations started at 404 Mc/s. The optical distribution is again seen to be narrower than the radio distributions.

Some of the details of the two distributions will now be discussed. The extension of the nebula to the south-west is clearly visible in the optical immersion curve between $01^h\,56^m$ and $02^h\,00^m$, just ahead of the rapid increase which occurs when the central region of the nebula is occulted between $02^h\,00^m$ and $02^h\,06^m$. It is not so prominent in the radio distribution, again indicating a reduced central concentration at radio wavelengths compared with optical wavelengths.

There is a peak in both the radio and optical distributions between $02^h\,04^m$ and $02^h\,06^m$, which seems to correspond to the strip that includes the optical maxima designated A, B, and C on Plate 1. On emersion there is a peak in all curves at about $02^h\,41^m$, corresponding to the uncovering of C, and steps at the uncovering of A and B at $02^h\,47^m$ and $02^h\,44^m$.

All three curves are in very good agreement in the period $02^h\,06^m$ to $02^h\,12^m$ as the north-east portion of the source is occulted. All curves show a minimum near $02^h\,07^m$, which coincides approximately with the occultation of the minimum in the brightness distribution near the double star and also with the bay to the east of the nebula. The minimum is more pronounced for the optical curve in the emersion.

During emersion, the most striking feature of the curves is the sharp peak in the optical distribution near $02^h\,37^m$ when D, the narrow central ridge elongated parallel to the limb of the Moon, is finally uncovered. No such prominent feature is visible on the radio distribution. This can also be seen during the immersion; at $02^h\,09^m$ there is an optical peak but no comparable radio effect as D is occulted. There is fair agreement between the optical and radio distribution as the south-eastern section of the nebula is uncovered.

(*d*) *Spectrum of the Crab Nebula*

In the previous sections, it was shown that the optical emission was more concentrated towards the centre of the nebula than the radio emission. The central optical feature D was scarcely visible at radio wavelengths, whereas the outer regions in the south were relatively more intense at radio than at optical wavelengths.

The variation of the optical-to-radio spectral index across the Crab nebula can be evaluated from the agreement already noted between the observed radio occultation curve and that of the square root of the observed optical brightness. If $S_{\text{radio}} = K(S_{\text{optical}})^{\frac{1}{2}}$, and if the spectrum of the flux of the emission is proportional to $f^{-\alpha}$, where α is the spectral index, then α decreases by $0{\cdot}16$ from the outer areas, where the optical brightness is 5, to the centre where it is 300.* The spectral index is thus higher in the outer regions than at the centre.

* The change $\Delta\alpha$ in spectral index is given by

$$\Delta\alpha = \frac{\log_{10}(300/5)^{\frac{1}{2}}}{\log_{10}(f_{\text{optical}}/f_{\text{radio}})} = 0{\cdot}16\,.$$

LUNAR OCCULTATION OF THE CRAB NEBULA

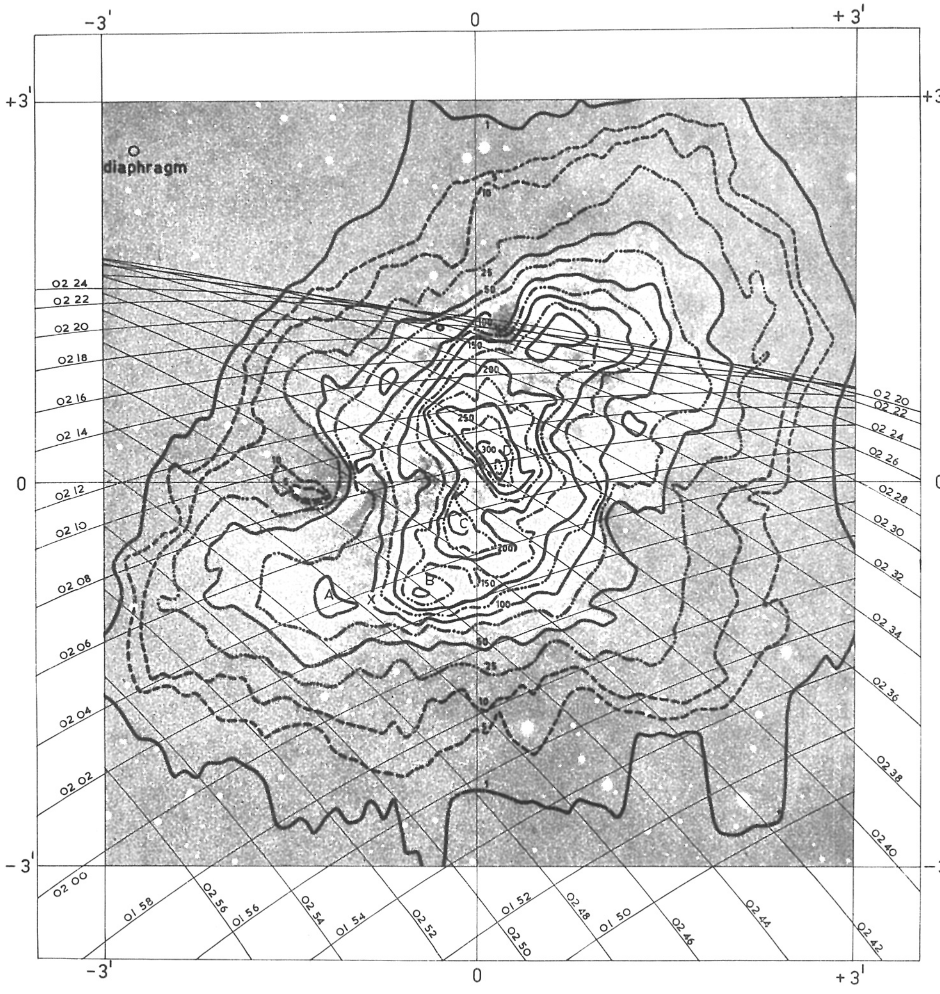

The passage of the Moon across the Crab nebula on June 21, 1963, showing the position of the upper limb of the Moon every 2 min of U.T. North-east is at the top left-hand corner. The optical brightness contours are reproduced from Woltjer (1957). The position of the 26 Mc/s source is shown X.

The variation in the spectral index over the nebula in the frequency range 404–1420 Mc/s can be studied from the derived distributions in Figure 5. The distributions at both immersion and emersion show that at about $02^{h}\,09^{m}$ and $02^{h}\,38^{m}$, when the central regions are being occulted, the 1420 Mc/s distribution lies slightly above the 404 Mc/s distribution but that, as we move away from the centre, in general the 404 Mc/s curve lies above the 1420 Mc/s curve. Thus, α becomes lower in the central regions. On the edge of the nebula where the 404 Mc/s intensity is 50% of its peak value, the 1420 Mc/s intensity is only 42% of its peak value. On evaluation, this indicates that at the half-intensity points the spectral index in the range 404–1420 Mc/s had increased by $0 \cdot 12$ relative to its value at the peak. If the spectral index of the whole source is taken as $\alpha = -0 \cdot 27$ (Conway, Kellermann, and Long 1963), then the central regions within the optical contour of 150 will have $\alpha = -0 \cdot 23$ and the outer regions will have $\alpha = -0 \cdot 35$.

At this point, it is appropriate to mention the small diameter steep-spectrum source in the Crab nebula observed at Cambridge by Hewish and Okoye (1964) and by Andrew, Branson, and Wills (1964). The position of their source lies between the bright regions A and B (Plate 1), which have been identified above with emitting regions at 404 and 1420 Mc/s. We do not see it, although it should have been easily visible if its intensity were 2% of the whole source, corresponding to the reported spectral index of $1 \cdot 2$. We thus infer that the spectrum must be even steeper. The Cambridge 404 Mc/s observations probably refer to another feature visible on the occultation curve. This is the extended source associated with the optical regions A and B, which probably consists of two parts each 20″–30″ in diameter. Its flux is $2 \cdot 0$% of the total at 404 Mc/s and $1 \cdot 5$% at 1420 Mc/s, and its spectrum is therefore much the same as the rest of the source.

(*e*) *Polarization of the 1420 Mc/s Emission from the Crab Nebula*

Figure 3(*a*) shows small changes in polarization as the outer extension of the source is occulted. This is followed by a rapid movement of the polarized intensity vector almost along a straight line from $02^{h}\,02^{m}$ to $02^{h}\,14^{m}$. During the emersion there is a similar movement in the reverse direction along a closely parallel line from $02^{h}\,25^{m}$ to $02^{h}\,44^{m}$. However, when the Moon's polarization, also shown in Figure 3(*a*), is subtracted to give Figure 3(*b*), it can be seen that the position angle during the immersion of about 100° differs by 20° from that of 80° during the emersion.

There may be a systematic error in removing the polarized contribution of the Moon (see subsection (*b*)), because the measurements, which were made at only four feed angles, probably contain a 360° angular period component. This would make the amplitude and position angle of the small residual polarization at the centre of the occultation rather inaccurate.

A reasonable interpretation of the rapid decrease and subsequent increase is that there is a central polarization concentration with a fairly constant position angle much the same as that of the whole source, which is $86° \pm 3°$. The best estimate of the degree of polarization of this concentration is $2 \cdot 5 \pm 0 \cdot 5$%, obtained by dividing the change in polarized intensity by the fractional change in total emission, compared with $1 \cdot 6 \pm 0 \cdot 15\%$ for the whole source. Within 5 min of the minimum of the occultation, the residual polarized intensity is about $0 \cdot 10 \pm 0 \cdot 05\%$, corresponding to a degree of polarization of $0 \cdot 5 \pm 0 \cdot 3\%$ for the unocculted northern region of the nebula. This supports the previous conclusion that the outer areas are weakly polarized relative to the central areas.

From the immersion and emersion time of $02^{\rm h}\,02^{\rm m}$ to $02^{\rm h}\,14^{\rm m}$ and $02^{\rm h}\,27^{\rm m}$ to $02^{\rm h}\,42^{\rm m}$ respectively, it appears that the polarization concentration is to the south-west of the centre of the nebula, which is similar to the result at 6 cm when measured with the 4′ arc beam of the 210 ft telescope (Gardner 1965). The 6 cm degree of polarization of over 15% is considerably greater than the $2 \cdot 5\%$ at 20 cm.

A comparison can be made of the changes of the observed position angle of the radio polarization with that of the optical polarization, which has been mapped in detail by Woltjer (1957) for regions where the optical brightness exceeds 50 units. The average optical position angle of the whole nebula is about 155°. The changes in position angle of the radio (Fig. 3(*b*)) and optical polarization over four intervals during the occultation can be summarized as follows.

(1) From $02^{\rm h}\,00^{\rm m}$ to $02^{\rm h}\,10^{\rm m}$, the optical position angle decreases by $8° \pm 5°$, while the radio position angle increases by $11° \pm 4°$.

(2) From $02^{\rm h}\,10^{\rm m}$ to $02^{\rm h}\,23^{\rm m}$, the optical position angle increases by $22° \pm 5°$, while the radio position angle increases by $30° \pm 15°$.

(3) From $02^{\rm h}\,23^{\rm m}$ to $02^{\rm h}\,37^{\rm m}$, the optical position angle increases by $19° \pm 5°$, while the radio position angle decreases by $60° \pm 20°$.

(4) From $02^{\rm h}\,37^{\rm m}$ to $02^{\rm h}\,49^{\rm m}$, the optical position angle decreases by $6° \pm 5°$, while the radio position angle decreases by $6° \pm 2°$.

It is evident that there is little detailed correspondence between optical and radio polarization even in the areas of strong polarization (1)–(4). Some of the disagreement for the interval (3) is probably due to the uncertainty of the position angle at the occultation minimum. As the weak south-eastern extension of the source is uncovered, large changes in radio polarization occur in the interval $02^{\rm h}\,50^{\rm m}$ to $03^{\rm h}\,10^{\rm m}$. Since the occultation had finished by $02^{\rm h}\,56^{\rm m}$, it is possible that the signal contained some partially polarized solar radiation, probably scattered from a local ground feature. In previous experience with polarization observations made in the daylight hours, such interference had generally lasted under 10 min, while the interval between occurrences was of the order of hours.

IV. Discussion and Conclusions

While most topics have been discussed in the individual sections concerned, the points that have been established with reasonable certainty will be summarized here.

(1) A feature of both the intensity and polarization occultation curves at radio wavelengths is the absence of any marked irregularities. The radio emission thus

appears to be smoothly distributed through the nebula like the polarized optical continuum radiation.

(2) There is good general agreement between optical and radio brightness distributions, and the centroids agree to within 4″ arc.

(3) The radio occultation curve shows the major features of the optical continuum features. The feature D on Plate 1 is, however, considerably more prominent at optical wavelengths.

(4) The spectral indices, optical-to-radio and also 1420-to-404 Mc/s, steepen towards the outside of the nebula. This indicates a corresponding change in the energy distribution of the synchrotron electrons, with a deficiency of high energy electrons in the outer envelope of the nebula.

(5) The low frequency (26 Mc/s) small diameter source was not seen at 404 Mc/s, although it should have been if the spectral index of 1·2, claimed by Cambridge, persisted to 400 Mc/s.

(6) There is no significant polarization at 404 Mc/s. However, differential Faraday rotation over the receiver bandwidth would severely reduce any monochromatic polarization present. The difference in position angle between the receiving bands at 394 and 414 Mc/s, corresponding to a rotation measure of -27 rad/m^2 (Gardner and Whiteoak 1963), is 85°. At 1420 Mc/s, the corresponding difference in angles is 6° and will have a negligible effect on the results.

(7) The 1420 Mc/s polarization is concentrated towards the centre of the nebula, with a degree of polarization of about 2·5% compared with 1·6% for the whole source. The main concentration appears to be located to the south-west of the centre of the nebula.

(8) There is no detailed correspondence between the position angle of the optical and radio polarization. Emission from different parts of the source may be subject to different amounts of depolarization at 21 cm while the optical emission is unaffected.

V. Acknowledgments

The authors are indebted to Mr. J. G. Bolton for his assistance, comments, and advice during the course of this work. One of us (C.H.) thanks Dr. E. G. Bowen for his invitation to carry out occultation work at Parkes as a guest observer from the School of Physics, University of Sydney.

VI. References

Andrews, B. H., Branson, N. J. B. A., and Wills, D. (1964).—*Nature* **203**: 171.

Conway, R. G., Kellermann, K. I., and Long, R. J. (1963).—*Mon. Not. R. Astr. Soc.* **125**: 261.

Gardner, F. F. (1965).—*Aust. J. Phys.* **18**: 385.

Gardner, F. F., and Whiteoak, J. B. (1963).—*Nature* **197**: 1162.

Hewish, A., and Okoye, S. E. (1964).—*Nature* **203**: 171.

Seeger, C. L., and Westerhout, G. (1957).—*Bull. Astr. Insts Neth.* **13**: 312.

Woltjer, L. (1957).—*Bull. Astr. Insts Neth.* **13**: 30.

Woltjer, L. (1958).—*Bull. Astr. Insts Neth.* **14**: 39.